

2024

Aqueous solutions of simple sugars. — Aqueous solutions of four simple sugars, α -D-glucose, β -D-glucose, α -D-mannose and α -D-galactose were investigated by ab initio molecular dynamics (AIMD) simulations. Hydrogen bonding (HB) properties were analyzed, including the number of hydrogen bond donors and acceptors, as well as the lengths and strengths of the hydrogen bonds between sugar and water molecules. Related electronic properties, such as the dipole moments of water molecules and partial charges of the sugar O-atoms, were calculated. The spatial distribution functions were used to characterize the hydrophilic and hydrophobic shells. It was observed that β -D-glucose forms the highest number of hydrophilic and the smallest number of hydrophobic connections to neighboring water molecules. The average hydrogen bond length in sugar-water was shortest for β -D-glucose, indicating that these hydrogen bonds are the strongest. Additionally, β -D-glucose stands out due to the symmetry properties of both its hydrophilic and hydrophobic hydration shells. In summary, in all aspects considered here, there seems to be a correlation between the distinct characteristics of β -D-glucose, which is one important factor associated with its outstanding solubility in water. [1]

Network structure of alcohols vs. T, p. —The cluster formation ability of two pure monohydroxy alcohols, namely the 2-ethyl-1-hexanol (2E1H) and 2-methyl-3-hexanols (2M3H) are studied via synchrotron x-ray diffraction and classical molecular dynamics simulations on wide temperature (between 163K and 413K) and pressure (between 0.1GPa and 3GPa) range (Figure 1). The simulation results are validated by the satisfactory agreement between the experimental and calculated structure factors. Based on the analysis of the configurations, the hydrogen-bonded network elements are categorized into monomer, ring, linear- and branched chain motifs. At room temperature, linear and branched chains dominate in 2E1H, while linear chains and rings in 2M3H. Generally, increasing temperature promotes linear chains and monomer structures, which are supported by the breaking of branched chains in 2E1H and rings in 2M3H. Interestingly, raising the pressure does not affect the probabilities of the different motifs in the 2M3H network, but linear chains start to form branched chains in 2E1H. [2]

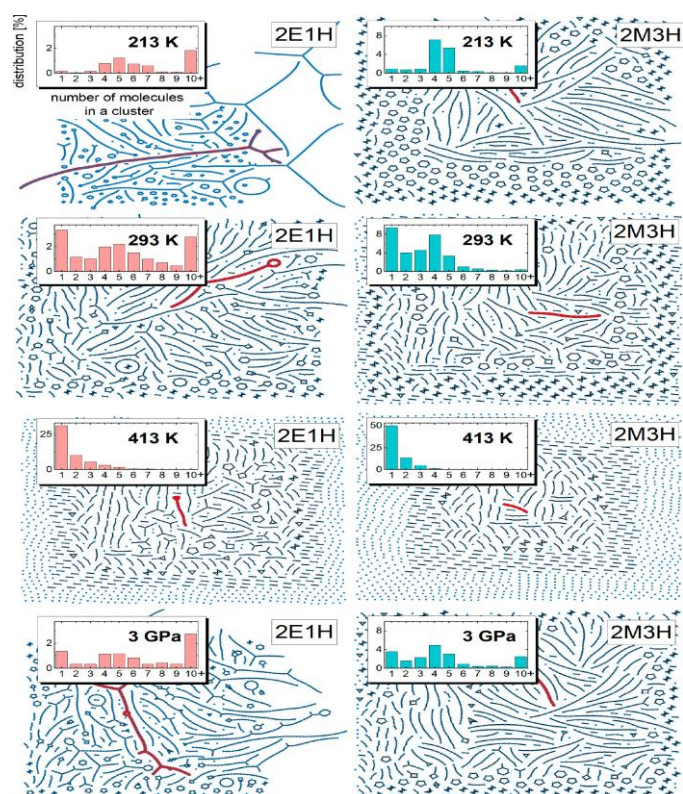


Figure 1. Visualization of lone and bonded hydroxyl groups derived from one configuration of simulation trajectory for 2E1H and 2M3H. The cluster colored in red is the largest one in the configuration. The insets show the histograms of the number of molecules in a cluster.[2]

Atomic structure and devitrification of vitreous $\text{Mg}_{82}\text{Ca}_8\text{Au}_{10}$. —Short range order of a ternary $\text{Mg}_{82}\text{Ca}_8\text{Au}_{10}$ biodegradable amorphous alloy was studied by combining diffraction datasets and Au L3 edge EXAFS data by the Reverse Monte Carlo simulation technique. It was found that while the Mg–Mg bond length agrees well with the empirical atomic diameter of Mg, both the Mg–Ca and Mg–Au mean interatomic distances are $\sim 9\%$ shorter than the sum of the corresponding atomic radii. The Ca–Au bond length exhibits $\sim 14\%$ shortening. The linear expansion coefficients of the glass determined from the temperature induced shift of the first peak of the structure factor and the reduced pair distribution function are $\sim 3.7 \times 10^{-5} \text{K}^{-1}$ and $\sim 3.1 \times 10^{-5} \text{K}^{-1}$, respectively. During devitrification, two crystalline phases emerge from the amorphous alloy: hexagonal AuMg_3 and the solid solution of Ca in hexagonal close packed Mg. The thermal expansion behaviour of the AuMg_3 unit cell was also determined using diffraction data. [3]

References (choose maximum 5 articles, each must begin with <https://>):

[1] <https://doi.org/10.3390/molecules29102205>

[2] <https://doi.org/10.1021/acs.jpcllett.4c000857>

[3] <https://doi.org/10.1016/j.jnoncrysol.2024.123157>

Connecting diffraction experiments diffraction experiment and network analysis tools: a general scheme for the study of hydrogen bonded networks. — A self-consistent scheme has been devised [1] that is applicable for revealing details of the microscopic structure of hydrogen-bonded liquids, including the description of the hydrogen-bonded network. The scheme starts with diffraction measurements, followed by molecular dynamics simulations. Computational results are compared with the experimentally accessible information on the structure, that is most frequently the total scattering structure factor. In the case of an at least semi-quantitative agreement between experiment and simulation, sets of particle coordinates from the latter may be exploited for revealing non-measurable structural details. Calculations of some properties concerning the hydrogen-bonded network have also been described, in the order of increasing complexity: starting with the definition of a hydrogen bond, first and second neighborhoods are described via spatial correlation functions. Attention is then turned to cyclic and non-cyclic hydrogen bonded clusters, before cluster size distributions and percolation are discussed. We would like to point out that, as a result of applying the novel protocol, these latter, rather abstract, quantities become consistent with diffraction data: it may thus be argued that the approach reviewed here is the first one that establishes a direct link between diffraction measurements and elements of network theories. Applications for liquid water, simple alcohols and alcohol-water liquid mixtures demonstrate the usefulness of the aforementioned characteristics [1]. The procedure can readily be applied to more complicated hydrogen bonded networks, like mixtures of polyols (diols, triols, sugars, etc...) and water, and complex aqueous solutions of even larger molecules (even of proteins).

On the Temperature- and Composition-Dependent Structure of Methanol/Water liquid mixtures. — The hydrogen-bonded structure of methanol – water mixtures has been investigated over the entire alcohol concentration range (from $x_{\text{Methanol}} = 0.1$ to 1.0) at several temperatures, from 300 K down to the freezing point of the given mixture [2]. Classical molecular dynamics simulations have been carried out, using the all-atom OPLS-AA force field for methanol and the TIP4P/2005 model for water molecules. Simulation trajectories ('particle configurations') obtained have been analyzed, in order to characterize the hydrogen-bonded network in the mixtures. The temperature and concentration dependence of the average hydrogen bond numbers between different types of molecules, the donor/acceptor roles of water and methanol molecules, and hydrogen bond number distributions have been revealed.

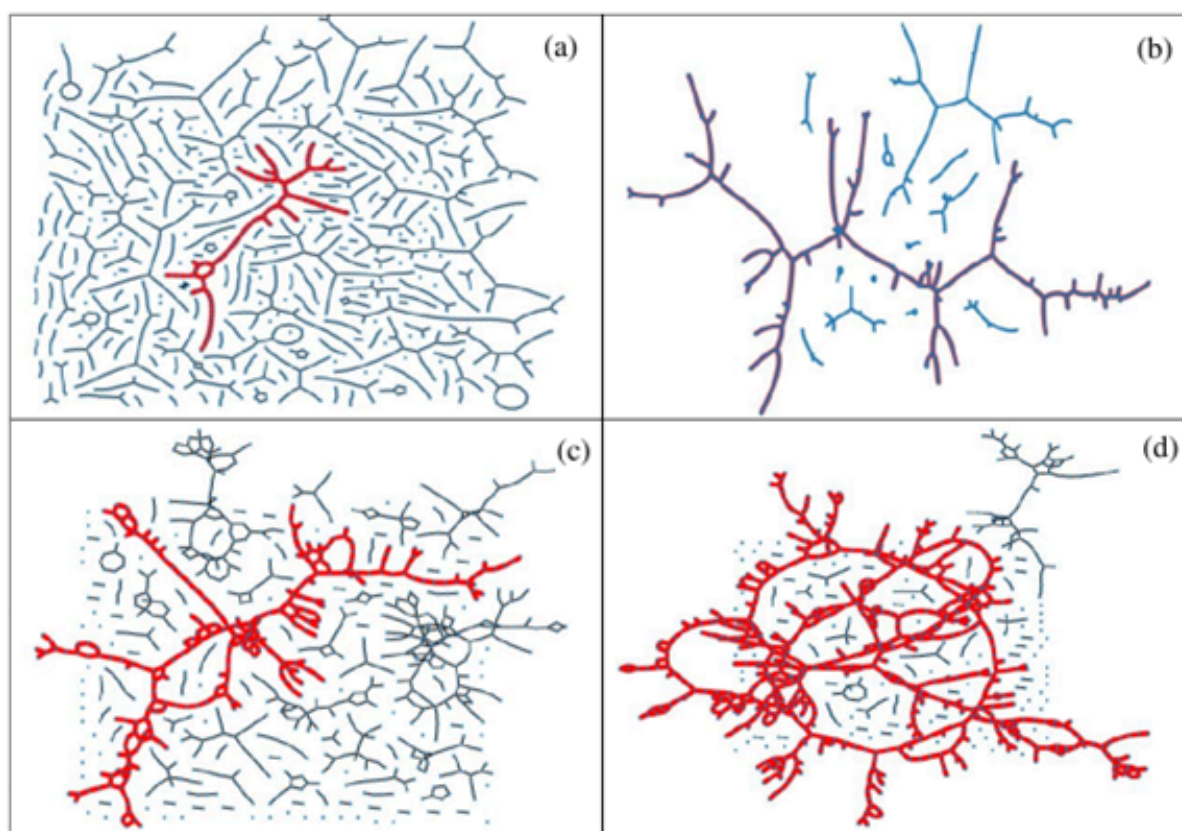


Figure 1. Typical H-bond topology of (a, b) pure methanol (a) at $T = 300$ K, and (b) at $T = 163$ K, and (c, d) of the water – subsystem in the methanol – water mixture of $x_M = 0.54$ (c) at $T = 300$ K, and (d) $T = 268$ K. Blue dots: molecules; black lines: H-bonds; red thick lines: H-bonds belong to the largest cluster.

The topology of the total system, as well as that of the water and methanol subsystems, has been investigated by calculating the cluster size distributions, the number of primitive rings, and ring size and ring type distributions.

The wide variation of cluster topologies may be followed in **Figure 1**. It has been found that upon cooling, the average number of H-bonded water molecules increases at every concentration and temperature investigated. As far as the connectivity of the hydrogen-bonded network is concerned, the percolation threshold has been shown to be above $x_M=0.9$ already at room temperature.

Short and medium range order of glassy KSb_5S_8 . — Glassy KSb_5S_8 was studied [3] by a number of experimental techniques and theoretical methods. In particular, the investigation included X-ray and neutron diffraction techniques, EXAFS and reverse Monte Carlo simulation, as well as DFT studies of clusters of various sizes. Various models of the glassy structure were analysed and compared with crystalline KSb_5S_8 . It was found that Sb atoms in the vitreous state are mostly threefold coordinated by S atoms with a significant contribution of higher coordination. The percentage of corner and edge sharing polyhedra and the distribution of bridging S atoms around Sb is similar in the crystalline and glassy states. DFT studies were used to explore a large number of clusters representative of neat Sb_2S_3 and KSb_5S_8 , in an effort to illuminate the role of K_2S in the Sb_2S_3 glass and account for the spectral features observed in Raman spectra. The main finding is that the addition of K_2S does not cause the typical modification observed in oxide glasses upon alkali oxide addition. The presence of K_2S seems to favor hypervalent bonding exemplified by the signature of quasi-tetrahedral units in Raman spectra.

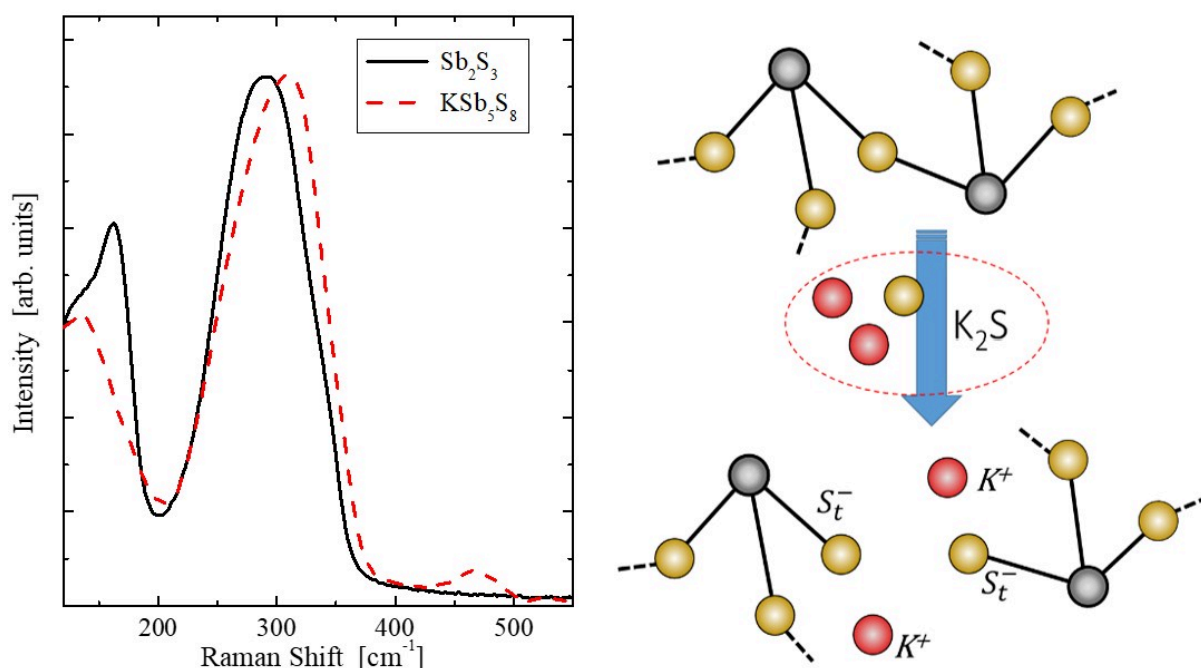


Figure 2. FT-Raman spectra of glassy Sb_2S_3 and KSb_5S_8 (left). The spectra have been normalized to the maximum band intensity for better comparison. Schematic illustration of the bridge breaking due to K_2S addition in Sb_2S_3 (right).

References:

- [1] Bakó, I.; Pothoczki, S.; Pusztai L.; Connecting Diffraction Experiments and Network Analysis Tools for the Study of Hydrogen-Bonded Networks, *The Journal of Physical Chemistry B* 127, 2023, 3109-3118; <https://doi.org/10.1021/acs.jpcc.2c07740>
- [2] Pethes, I; Pusztai, L; Temleitner, L; Evolution of the hydrogen-bonded network in methanol-water mixtures upon cooling; *J. Mol. Liquids* 386, 2023, 122494; <https://doi.org/10.1016/j.molliq.2023.122494>
- [3] Jóvári, P; Chrissanthopoulos, A; Andrikopoulos, KS; Pethes, I; Kaban, I; Kohara, S; Beuneu, B; Yannopoulos, SN; Short range order of glassy KSb_5S_8 by diffraction, EXAFS, vibrational spectroscopy and DFT calculations; *J. Non-Cryst. Solids* 616, 2023, 122461; <https://doi.org/10.1016/j.jnoncrysol.2023.122461>

The structure of concentrated aqueous cesium chloride solutions – revisited. — The structure of aqueous CsCl solutions was investigated by classical molecular dynamics simulations (MD) at three salt concentrations (1.5, 7.5, and 15 mol %) [1]. Thirty interatomic potential sets, based on the '12–6 Lennard-Jones plus Coulomb' model, parametrized for non-polarizable water solvent molecules, were collected and tested. Some basic properties, such as density, static dielectric constant, and self-diffusion coefficients, predicted by the force fields (FF), were compared with available experimental data. The simulated particle configurations were used to calculate the partial radial distribution functions (PRDF) and the neutron and X-ray total scattering structure factors (TSSF). The TSSFs were compared with experimental data from the literature, to find the best FF models, which describe the structure correctly. It was found that, though several of the thirty models failed in the tests, some models are compatible with the measured data. Values of the structural parameters consistent with the experiments were determined (such as water-ion distances, the average number of water molecules around the ions, average number, and distance between anion-cation contact ion pairs, water-water hydrogen bonds). It was shown that in addition to models in which the number of contact ion pairs is too high, models in which this number is too low are also unable to reproduce experimental data.

Structural studies of ^1H -containing liquids by polarized neutrons: chemical environment and wavelength dependence of the incoherent background. — Following a demonstration of how neutron diffraction with polarization analysis may be applied for the accurate determination of the coherent static structure factor of disordered materials containing substantial amounts of proton nuclei (Temleitner et al., Phys. Rev. B 92, 014201, 2015), we now focus on the incoherent scattering. Incoherent contributions are responsible for the great difficulties while processing standard (non-polarized) neutron diffraction data from hydrogenous materials, hence the importance of the issue. Here we report incoherent scattering intensities for liquid acetone, cyclohexane, methanol and water, as function of the $^1\text{H}/\text{H}$ ratio. The incoherent intensities are determined directly by polarized neutron diffraction. This way, possible variations of the incoherent background due to the changing chemical environment may be monitored. In addition, for some of the water samples, incoherent intensities as a function of the wavelength of the incident neutron beam (at 0.4, 0.5 and 0.8 Å) have also been measured. It is found that in each case, the incoherent intensity can be described by a single Gaussian function, within statistical errors. The (full) width (at half maximum) of the Gaussians clearly depends on the applied wavelength. On the other hand, the different bonding environments of hydrogen atoms do not seem to affect the width of the Gaussian. [2]

On the Temperature- and Pressure-Dependent Structure of Liquid Phosphorus. — Apart from the well-known molten white phosphorus, existing at temperatures around 50 °C under atmospheric pressure, early in this millennium, new high- pressure, high-temperature phases have been discovered. One group of the newly found liquids can be identified as being formed by P_4 molecules, just like common molten white phosphorus. The structures of these (“old” and “new”) forms have not yet been compared in detail: this comparison is in the focus of the present work [3]. It has been demonstrated that the tetrahedral shape of the molecules may be maintained in all three liquids considered, see Figure 1. Orientational correlations between P_4 tetrahedra, as a function of the distance between centers of tetrahedra, have been revealed. It is found that face-to-face type contacts occur at much lower center–center distances in the newly discovered liquids. As an addition, new estimates, based on series of Reverse Monte Carlo calculations, for the densities of the high-temperature phases are provided; this step is necessary because in this respect, sizeable uncertainties have been reported previously.

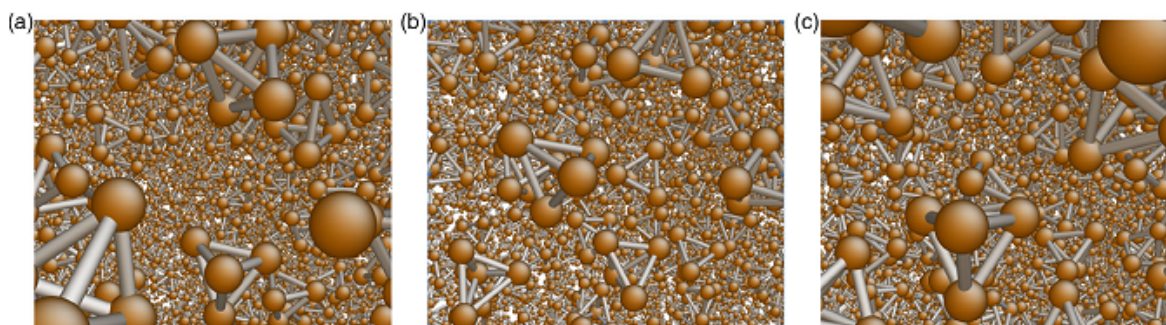


Figure 1. Snapshots of RMC particle configurations for A) ambient white P_4 , as well as black P_4 at B) 0.77 GPa and C) 0.96 GPa. Note the nearly perfect tetrahedral molecules in each system.

Topology of network glasses. — The structural properties of two Ge-As-Se glass compositions ($\text{Ge}_{10}\text{As}_{10}\text{Se}_{80}$ and $\text{Ge}_{21}\text{As}_{21}\text{Se}_{58}$) are investigated from a combination of density-functional-based molecular dynamics simulations and neutron/x-ray scattering experiments. Various properties of the resulting particle configurations (see Figure 2.) are analysed, including structure factors, pair distribution functions, angular distributions, coordination numbers, and neighbor distributions, and compare our results with the experimental data. Results leave anticipated coordinations from the octet rule (Se^{II} , As^{III} , and Ge^{IV}) unchanged, and these are contrasted with respect to glasses having similar average coordination number $\langle r \rangle$ such as binary $\text{As}_{30}\text{Se}_{70}$ and $\text{Ge}_{33}\text{Se}_{67}$. The increase of (As,Ge) content induces a growth of ring structures that are dominated by edge-

sharing motifs (four-membered rings) having mostly heteronuclear bonds, while As-As and As-Ge homonuclear bonds are clearly more favored than Ge-Ge. These features signal that both topological (rings) and chemical (bonds) features are different with respect to related binaries. The validity of the so-called vibrational isocoordination rule stating that properties of multicomponent chalcogenides depend solely on $\langle r \rangle$ is checked, and results from a vibrational analysis indicates that this rule is merely satisfied for the Se-rich composition. An inspection of correlations via the Bhatia-Thornton formalism shows that topological ordering is not only different between $\text{Ge}_{10}\text{As}_{10}\text{Se}_{80}$ and $\text{Ge}_{21}\text{As}_{21}\text{Se}_{58}$ but also radically contrasts with respect to the isocoordinated binary glasses and displays an obvious reduced directional bonding. [4]

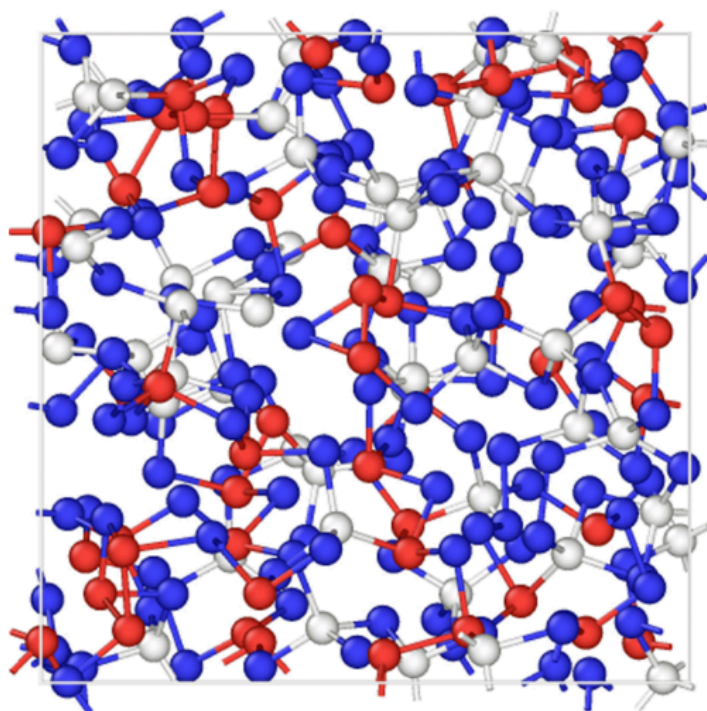


Figure 2. An example of an obtained amorphous $\text{Ge}_{21}\text{As}_{21}\text{Se}_{58}$ system. Blue, white, and red atoms represent selenium, germanium, and arsenic atoms, respectively.

2021

Temperature-dependent structure of alcohol–water liquid mixtures. — Our group is in the midst of a long-term systematic investigation in this field; as next steps, experimental and simulated results have been published for ethanol–water [1] and 1- and 2-propanol–water mixtures [2, 3]. Experimentally, these mixtures have been investigated by high energy synchrotron X-ray and neutron diffraction at low temperatures. It was thus possible to report the first complete sets of X-ray weighted total scattering structure factors over the entire composition range (at many different ethanol (x_{Et}) and 1- and 2-propanol concentrations ($x_{1\text{Pr}}$ and $x_{2\text{Pr}}$, respectively) from 10 to 100 mol%, or mole fractions between 0.1 and 1.0) and at temperatures from ambient down to the freezing points of the mixtures. The new diffraction data may later be used as reference in future theoretical and simulation studies. Measured data were interpreted by molecular dynamics simulations, in which the all-atom OPLS/AA force field model for ethanol, 1-propanol and 2-propanol were combined with both the SPC/E and TIP4P/2005 water potentials. Both combinations provide at least semi-quantitative agreement with measured diffraction data. As a general trend, the average number of hydrogen bonds increases upon cooling. For ethanol–water mixtures, it was found that 5-membered hydrogen bonded cycles are dominant up to an ethanol mole fraction of $x_{\text{Et}}=0.7$ at room temperature, above which concentration ring structures nearly disappear. It could be shown that at low temperature, close to the freezing point even the mixture with 90% ethanol ($x_{\text{Et}}=0.9$) possesses a 3D percolating network. Moreover, the water sub-network also percolates even at room temperature, with a percolation transition occurring around $x_{\text{Et}}=0.5$. For 1-propanol–water mixtures, strong temperature dependence of the percolation threshold, as well as of the participation of the number of doubly hydrogen bonded molecules in cyclic entities, have been found for the mixture with 89 mol % of 1-propanol. Above a 1-propanol content of 20 mol %, 5-fold rings are the most frequent cyclic entities, with a strong temperature dependence in terms of the number of rings. Finally, for 2-propanol–water mixtures, the percolation threshold at room temperature could be estimated to be between isopropanol concentrations of 62 and 74 mol %, whereas at very low temperature, calculations yielded a value above 90 mol %. Figure 1 displays typical hydrogen bond topologies in 2-propanol–water mixtures, as a function of temperature and composition.

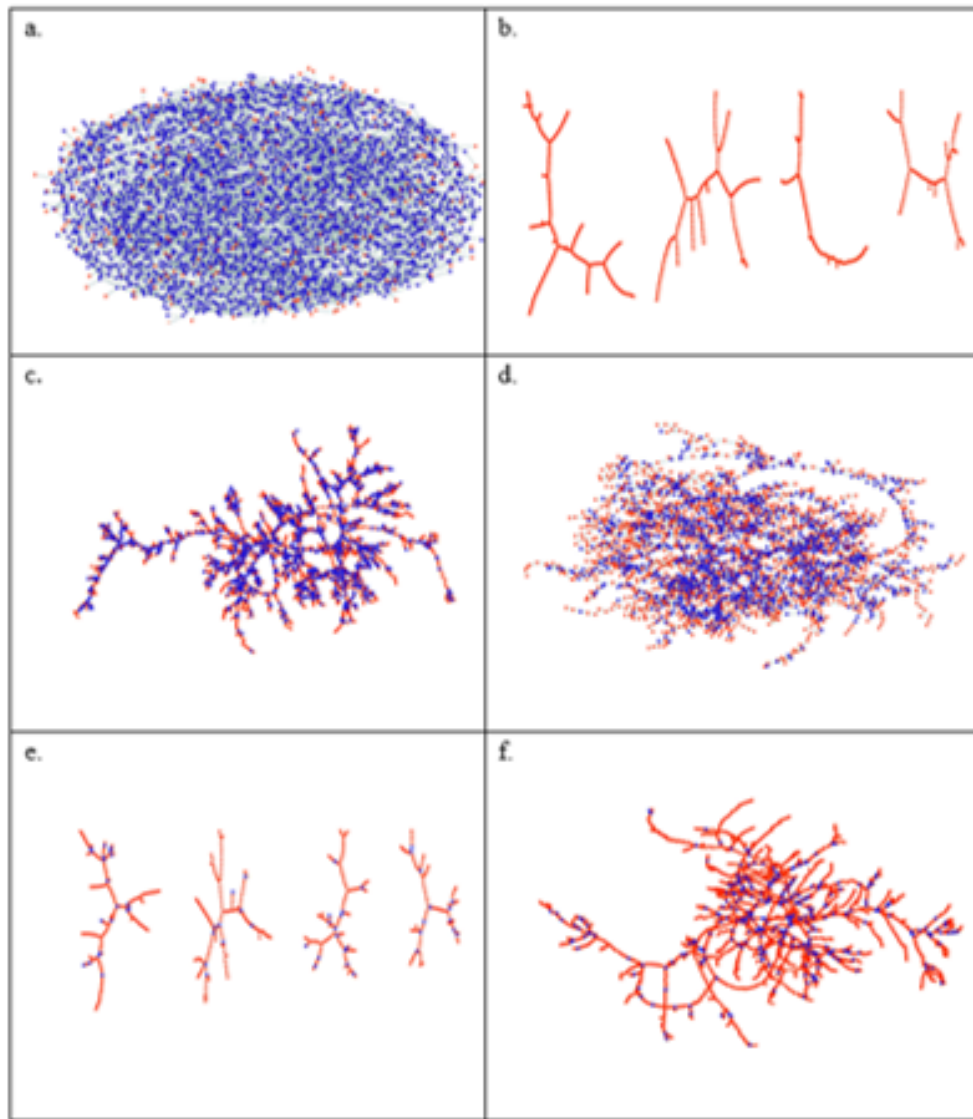


Figure 1. Typical hydrogen-bond topologies a) $x_{2Pr}=0.1$ at 230 K, b) pure isopropanol at 230 K, c) $x_{2Pr}=0.62$ at 298 K, d) $x_{2Pr}=0.62$ at 230 K, e) $x_{2Pr}=0.9$ at 298 K, f) $x_{2Pr}=0.9$ at 230 K.

Short range order in a biocompatible metallic glass. — Metallic materials have long been used to help repair or replace diseased or damaged bone tissue. Current metallic biomaterials (stainless steels, cobalt-based alloys, titanium-based alloys) are permanent fixtures, which in the forms of plates, screws and pins help to secure fractures and must be removed by a second surgical procedure after the tissue has healed sufficiently. To avoid the post-extraction intensive efforts are being made in recent years to develop new classes of so-called “biodegradable implants”, composed of non-toxic materials that become reabsorbed by the human body after a reasonable period of time.

Biocompatible Mg-Zn-Ca alloys are corroded by the body fluids. The rate of corrosion/absorption can be tuned by the composition what makes them promising candidates for biodegradable implants. The structure of glassy $Mg_{66}Zn_{30}Ca_4$ was investigated by X-ray and neutron diffraction [4]. Large scale structural models were obtained by fitting X-ray and neutron diffraction structure factors simultaneously by the reverse Monte Carlo simulation method. Models were analysed at the level of pair correlations, free volume distribution and coordination polyhedra. It was found that the Zn-Zn partial pair correlation function has a sharp first peak with a deep minimum. The first minima of Mg-Zn and Zn-Ca partial pair correlation functions are also relatively deep suggesting a well-defined and compact coordination environment around Zn atoms. Delaunay analysis was used to investigate free volume distribution. Densely packed coordination polyhedra are significantly more frequently centred by Zn than by Mg (Figure 2). The clustering of well defined, densely packed Zn-centred polyhedra may hinder the rearrangement needed for crystallization and thus enhance the glass forming ability of $Mg_{66}Zn_{30}Ca_4$.

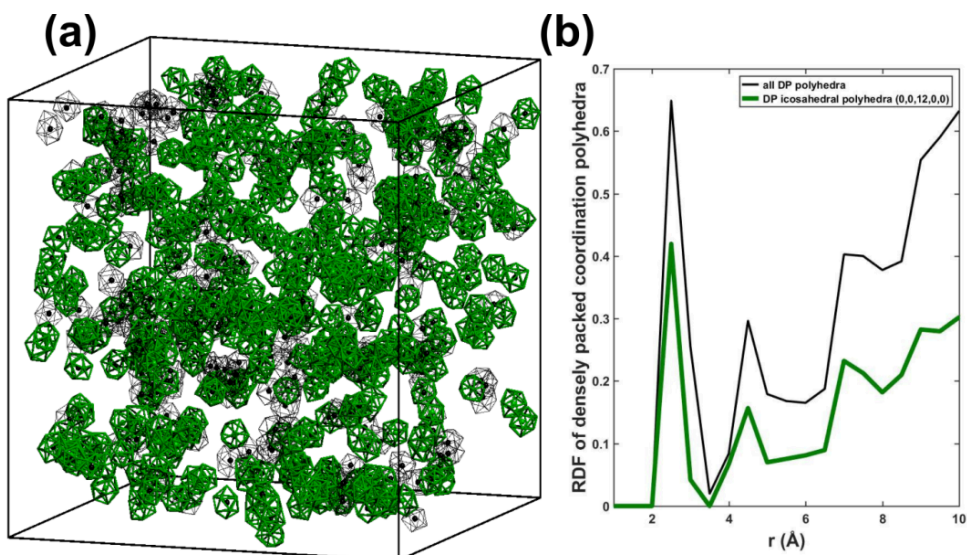


Figure 2. (a) Distribution of the densely packed (DP) polyhedra, by green are marked those with icosahedral arrangement (b) radial distribution function (RDF) of all the densely packed polyhedral (black) and those of icosahedral atomic arrangement.

A new method to characterize the local order of disordered phases. — For high symmetry molecules, a novel method has been presented, which describes orientational correlations between adjacent and distant pairs of molecules without any restriction to use on crystalline or liquid phases. The method has been generalized from an algorithm developed for tetrahedral molecules. In the original algorithm a given orientation of a pair of tetrahedral molecules is characterized unambiguously by the number of ligand atoms that can be found between two planes containing molecular centres and perpendicular to the centre-centre connecting line. In the generalized algorithm, the planes are replaced by cones. The apex angle of the cones are set to contain 2 ligand atoms of the molecule on average. To demonstrate the applicability of the method, the octahedral-shaped SF₆ molecule is studied in a wide range of phases (gaseous, supercritical fluid, liquid and plastic crystalline) using classical molecular dynamics. After the best performing forcefield has been found against density and neutron total scattering structure factors available in the literature, the orientational correlation analysis revealed a close-contact region in the first coordination shell and a medium-range order behaviour in the non-crystalline phases. While the former is invariant to changes of density, the latter showed longer-ranged correlations as density is raised. In the plastic crystalline state, fluorine atoms are oriented along with the lattice directions with higher probability. To test the method for icosahedral symmetries, the crystalline structures of room temperature C₆₀ is generated by three sets of potentials that produce different local arrangements. The novel analysis provided quantitative results on preferred arrangements for the first and second neighbours [5].

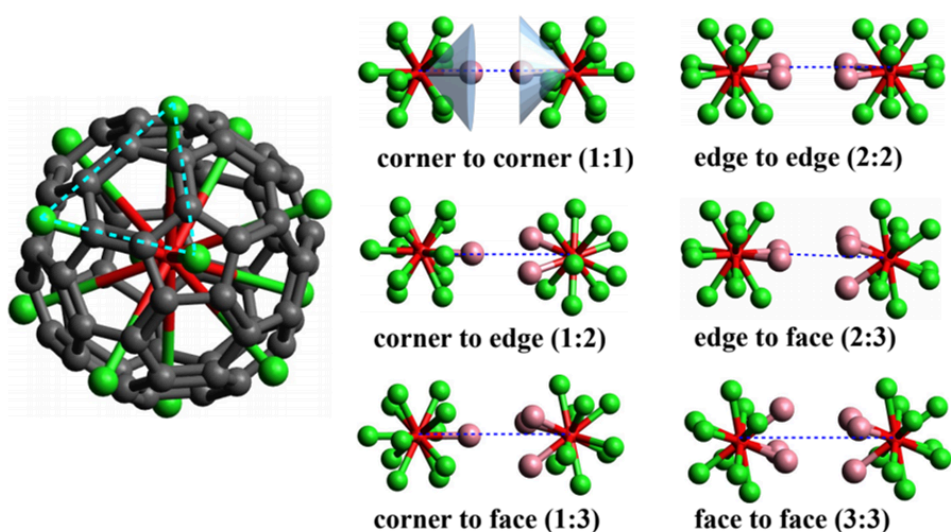


Figure 3. Classification of orientational correlations for pairs of icosahedra (left). The half apex angle of the orientation cone is 48.19° and the ligand atoms (green) inside the cones are highlighted with magenta. Based on the reconstruction of the icosahedral symmetry of the C₆₀ molecule (left), corners, edges and faces correspond to pentagonal face, double-bond (edge between two hexagonal faces) and hexagonal face, respectively.

References:

- [1] Pothoczki, S; Pethes, I; Pusztai, L; Temleitner, L; Ohara, K; Bakó, I; Properties of Hydrogen-Bonded Networks in Ethanol–Water Liquid Mixtures as a Function of Temperature: Diffraction Experiments and Computer Simulations; *The Journal of Physical Chemistry B*; 125(23), 6272-6279 (2021)
- [2] Pethes, I; Pusztai, L; Ohara, K; Temleitner, L; Temperature-dependent structure of 1-propanol/water mixtures: X-ray diffraction experiments and computer simulations at low and high alcohol contents; *J. Mol. Liq.*, 340, 117188, (2021);
- [3] Pothoczki, Sz; Pethes, I; Pusztai, L; Temleitner, L; Csókás, D; Kohara, S; Ohara, K; Bakó, I; Hydrogen bonding and percolation in propan-2-ol – Water liquid mixtures: X-ray diffraction experiments and computer simulations; *J. Mol. Liq.* 329 Paper:115592, 10 p. (2021);
- [4] Saksl, K; Pethes, I; Jóvári, P; Molčanová, Z; Ďurišin, J; Ballóková, B; Temleitner, L; Michalik, Š; Šulíková M et al. Atomic structure of the Mg₆₆Zn₃₀Ca₄ metallic glass. *J. Non-Cryst. Solids* 558 Paper: 120660, 9 p. (2021)
- [5] Temleitner, L; A generalized scheme for characterizing orientational correlations in condensed phases of high symmetry molecules: SF₆ and C₆₀; *J. Mol. Liq.*, 341, 116916, (2021);

2020

Solvent-separated anion pairs in concentrated solutions. — Hydrogen bonding to chloride ions in various aqueous environments has been discussed many times over the past more than 5 decades. Still, the possible role of such anion-to-water type hydrogen bonds (HB) in networks of HB-s has not been investigated in any detail. Here, computer models of concentrated aqueous LiCl solutions are considered and usual HB network characteristics, such as distributions of cluster sizes and of cyclic entities, are computed for the models by (1) taking and (2) not taking chloride ions into account. During the analysis of hydrogen bonded rings, a significant amount of ‘solvent separated anion pairs’ (see Fig.1) have been detected at high LiCl concentrations. It is demonstrated that including the halide anions into the network does make the interpretation of structural details significantly more meaningful than when considering water molecules only. Finally, simulated structures generated by ‘good’ and ‘bad’ potential sets have been compared on the basis of the tools developed here, and it is shown that the novel concept (1) is, indeed, helpful from this respect, too. [1]

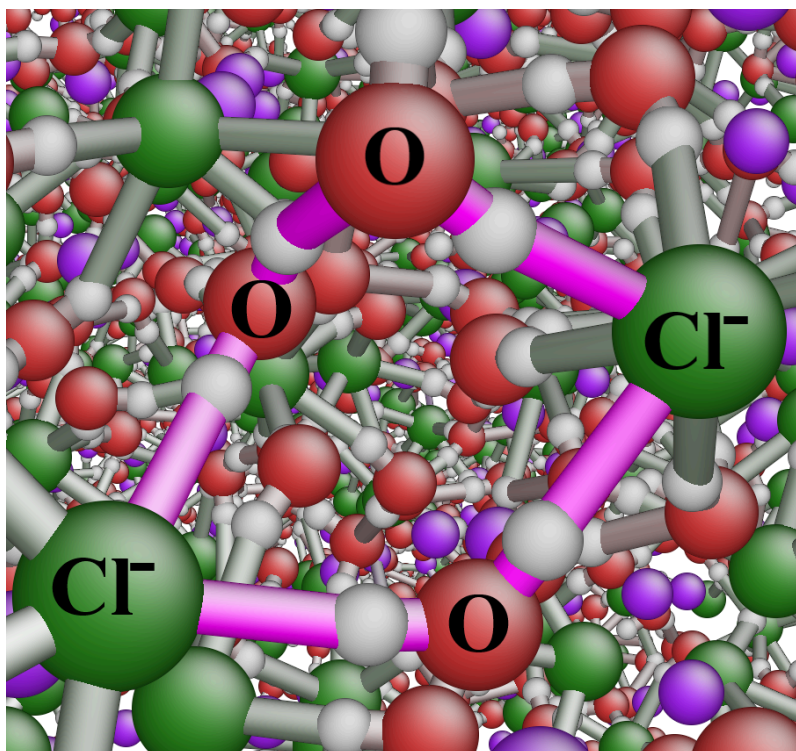


Figure 1. Snapshot of a simulated particle configuration with a very high LiCl concentration of 19.55 mol/kg. A 5-membered ring is in the front, with 2 Cl⁻ ions and 3 water molecules; the two anions are separated by a water molecule, i.e., the anions are ‘solvent-separated’.

Temperature-dependent structure of alcohol–water liquid mixtures. — Our group is in the midst of a long-term systematic investigation in this field; as a first step, experimental and simulated results have been

published [2] for methanol-water mixtures. Experimentally, these mixtures have been investigated by high-energy synchrotron X-ray and neutron diffraction at low temperatures. It was thus possible to report the first complete sets of both X-ray and neutron weighted total scattering structure factors over the entire composition range (at 12 different methanol concentrations (x_M) from 10 to 100 mol%) and at temperatures from ambient down to the freezing points of the mixtures. The new diffraction data may later be used as reference in future theoretical and simulation studies. Measured data were interpreted by molecular dynamics simulations, in which the all atom OPLS/AA force field model for methanol was combined with both the SPC/E and TIP4P/2005 water potentials. Both combinations provide at least semi-quantitative agreement with measured diffraction data. As a general trend, the average number of hydrogen bonds increases upon cooling. However, the number of hydrogen bonds between methanol molecules slightly decreases with lowering temperatures in the concentration range between ca. 30 and 60 mol % alcohol content. The same is valid for water-water hydrogen bonds above 70 mol % of methanol content, from room temperature down to 193 K.

Short range order and topology of Ge-Ga-Te glasses. — Due to their broad infrared transmission window glassy tellurides are extensively used in various fields of IR optics. The general strategy to find tellurides with excellent glass forming ability is to alloy the prototype Ge-Te system with a third component. Glasses with Ge-X-Te ($X = \text{Ga, As, Se, I, Ag, AgI}$) composition often possess a broad supercooled liquid region that makes it possible to shape bulk infrared lenses or draw fibers transmitting up to at least 18 μm . Structural background of glass forming of $\text{Ge}_x\text{Ga}_x\text{Te}_{100-2x}$ ($x = 7.5, 10, 12.5, 14.3$) glasses was investigated by diffraction techniques and EXAFS [3]. Models were obtained by fitting experimental datasets simultaneously in the framework of the reverse Monte Carlo simulation technique. It was shown that Ga and Ge atoms are mostly fourfold coordinated while N_{Te} , the average coordination number of Te increases with Ga content ($N_{\text{Te}} = 2.35 \pm 0.1$ for $x = 14.3$). The majority of Ge/Ga atoms are linked to other Ge/Ga atoms via one or two common Te neighbors forming corner and edge sharing tetrahedra.

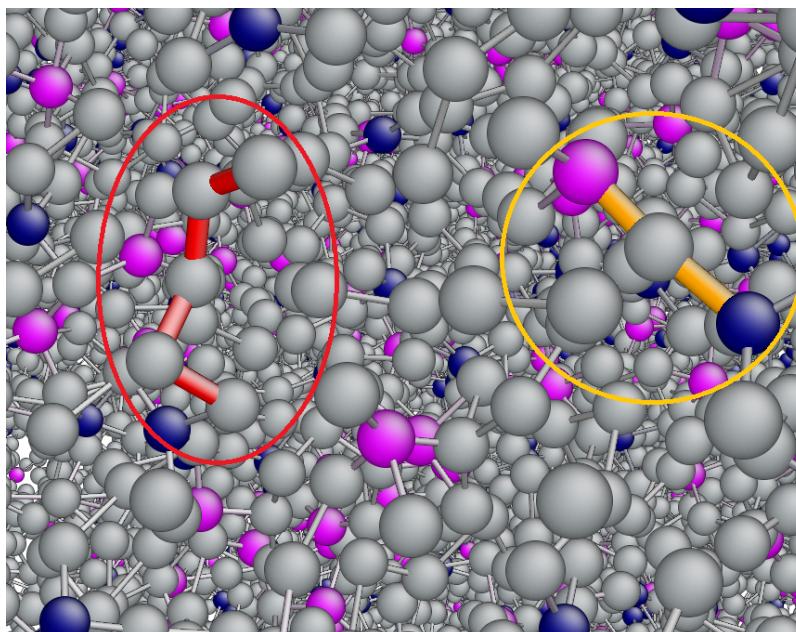


Figure 2. Part of the model of the $\text{Ge}_{7.5}\text{Ga}_{7.5}\text{Te}_{85}$ glass obtained by RMC simulation. The Ge, Ga and Te atoms are represented by magenta, blue and grey balls, respectively. Two corner sharing tetrahedra are marked with orange, a short chain of Te atoms is highlighted by red

References:

- [1] Pethes, I.; Bakó, I.; Pusztai, L. Chloride ions as integral parts of hydrogen bonded networks in aqueous salt solutions: the appearance of solvent separated anion pairs. *PHYSICAL CHEMISTRY CHEMICAL PHYSICS* 22 : 19 pp. 11038-11044. , 7 p. (2020)
- [2] Pethes, I.; Pusztai, L.; Ohara, K. ; Kohara, S. ; Darpentigny, J. ; Temleitner, L. Temperature-dependent structure of methanol-water mixtures on cooling: X-ray and neutron diffraction and molecular dynamics simulations. *JOURNAL OF MOLECULAR LIQUIDS* 314 Paper: 113664 , 10 p. (2020)
- [3] Pethes, I. ; Piarristeguy, A. ; Pradel, A. ; Michalik, S. ; Nemausat, R. ; Darpentigny, J.; Jóvári, P. Short range order and topology of $\text{Ge}_x\text{Ga}_x\text{Te}_{100-2x}$ glasses. *JOURNAL OF ALLOYS AND COMPOUNDS* 834 Paper: 155097 , 9 p. (2020)

Short range order and topology of Ge-Te glasses. — Detailed knowledge of the structure of binary Ge-Te glasses is useful in the structural investigations of more complex telluride glasses used in infrared optics or information technology. A thorough experimental study may also inspire theoreticians by providing them with reliable structural models. The structure of $\text{Ge}_x\text{Te}_{100-x}$ ($x = 14.5, 18.7, 23.6$) glasses prepared by twin roller quenching technique was investigated by neutron diffraction, X-ray diffraction and Ge-K-edge X-ray absorption spectroscopy measurements. Large scale structural models were obtained for each composition by fitting the experimental datasets in the framework of the reverse Monte Carlo technique [1]. It was found that the majority of Ge and Te atoms satisfy the 8-N rule. Simulation results indicate that Ge-Ge bonding is not significant for $x = 14.5$ and 18.7 . The shape and position of the first peak of the Ge-Ge partial pair correlation function evidence the presence of corner sharing tetrahedra already in compositions ($x = 14.5$ and 18.7) where 'sharing' of a Te atom by two Ge atoms could be avoided due to the low concentration of Ge (see Fig. 1).

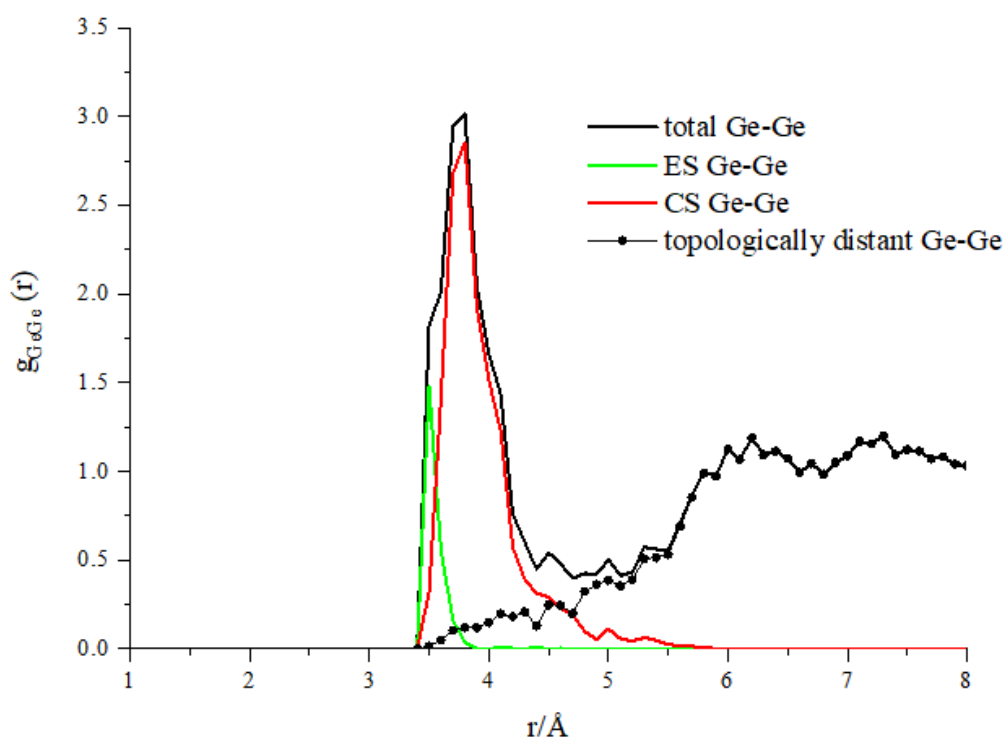


Figure 1. Decomposition of the first peak of $g_{\text{GeGe}}(r)$ of $\text{Ge}_{18.7}\text{Te}_{81.3}$ to contributions from corner sharing (CS) tetrahedra, edge sharing (ES) tetrahedra and topologically distant Ge-Ge pairs.

Structure and dynamics of isopropanol-water liquid mixtures. — Series of molecular dynamics simulations for 2-propanol–water mixtures, as a function of temperature (between freezing and room temperature) and composition (molar fraction of isopropanol, x_{ip} : 0, 0.5, 0.1, and 0.2), have been performed for temperatures reported in the only available experimental structure study. It is shown that, when the all-atom optimized potentials for liquid simulations (OPLS) interatomic potentials for the alcohol are combined with the TIP4P/2005 water model, near-quantitative agreement with measured X-ray data, in the reciprocal space, can be achieved [2]. Such an agreement justifies detailed investigations of structural, energetic, and dynamic properties on the basis of simulation trajectories. Here, the focus was placed on characteristics related to hydrogen bonds (HB): cluster-, and in particular, ring formation, energy distributions, and lifetimes of HB-s have been scrutinized for the entire system, as well as for the water and isopropanol subsystems. It is demonstrated that, similar to ethanol–water mixtures, the occurrence of 5-membered-hydrogen-bonded rings are significant, particularly at higher alcohol concentrations. Concerning HB energetics, an intriguing double maximum appears on the alcohol–alcohol HB energy distribution function. HB lifetimes have been found significantly longer in the mixtures than they are in pure liquids. As seen in Figure 2a, the local order of water molecules in the first shell is clearly a tetrahedral one. If we plot the energy distribution function on this surface (first shell), an attractive interaction between -3.0 and -6.0 kcal/mol is found. On the other hand, the first shell around O atoms of 2-propanol molecules appears in the H-bond donor and acceptor directions, but the structure of the second shell is not much ordered (Figure 2b). Concerning Figure 2c,d, the typical tetrahedral spatial distribution of neighbors (in the 1st and 2nd shells) around water molecules is clearly preserved also at a lower temperature (at 258 K).

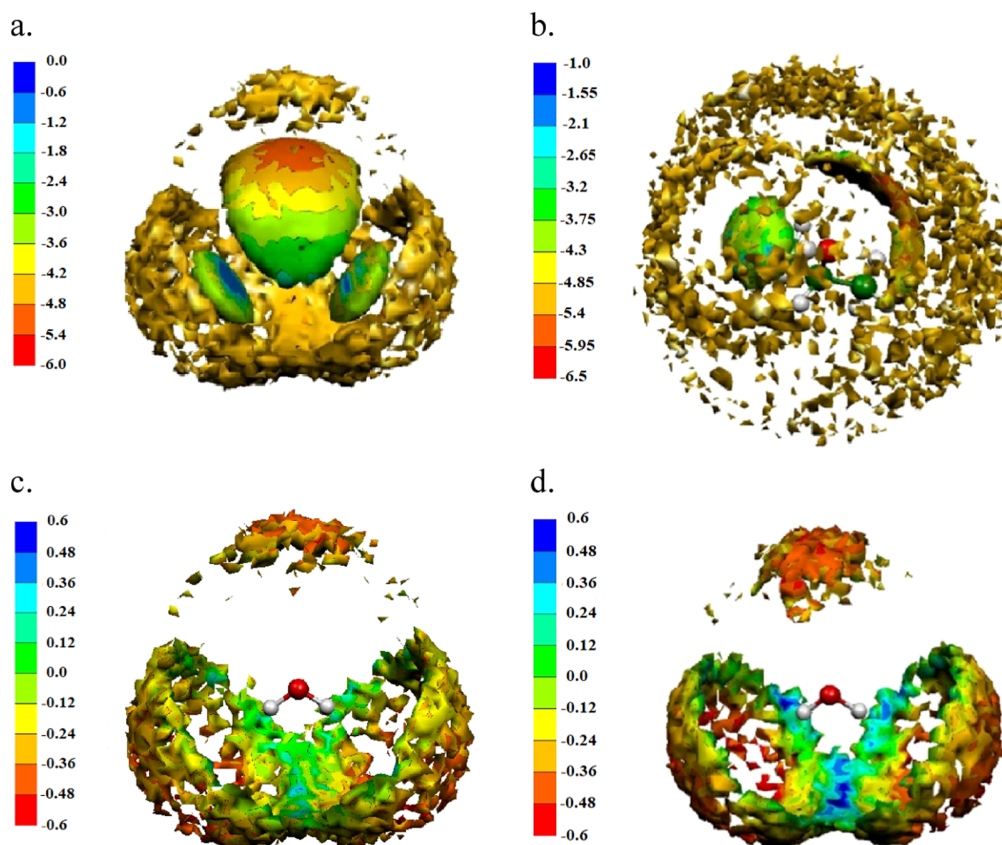


Figure 2. (a) First and second shells of the space density distribution (SDD) for water around water at 298 K. (Water–water energy distribution function (EDF) is represented by the color scale only in the case of the First shell). (b) First and second shells of the SDD for 2-propanol around 2-propanol at 298 K. (2-Propanol–2-propanol EDF is represented by the color scale only in the case of the First shell.) (c) second shell of the SDD for water around water at 298 K (water–water EDF is represented by color coding). (d) second shell of the SDD for water around water at 258 K (water–water EDF is represented by color coding). All results are shown for $x_{ip} = 0.2$.

External links:

[1] <https://doi.org/10.1016/j.jallcom.2018.08.323>

[2] <https://doi.org/10.1021/acs.jpcc.9b05631>

2018

Understanding disordered structures. — Our research group is involved in the investigation of short range order of liquids, amorphous materials and disordered crystals. We combine experimental data, such as X-ray and neutron diffraction structure factors and EXAFS spectra, with computer modeling tools, such as Reverse Monte Carlo (RMC) and molecular dynamics (MD) simulations. As a result of such an approach, large configurations (typically tens of thousands of atoms) are provided that are energetically reasonable and consistent (within errors) with experimental data. These configurations are then subjected to various geometrical analyses, so that specific questions concerning the structure of a material may be answered. The group is also responsible for the maintenance and operation of the MTEST neutron diffractometer installed at the 10 MW Budapest Research Reactor. Below we provide some selected results from the year of 2018.

Covalent glasses. — Short range order of $As_{40-x}Cu_xTe_{60}$ ($x = 0, 10, 20, 25, 30$) glasses has been studied by neutron- and X-ray diffraction, combined with extended X-ray absorption fine structure (EXAFS) measurements at the K-edges of all components. Large-scale structural models have been generated by fitting the experimental datasets simultaneously in the framework of the reverse Monte Carlo simulation technique. These simulations revealed that As and Te atoms bind to about 3 and 2 As/Te neighbors, respectively, both of which possess Cu neighbors.

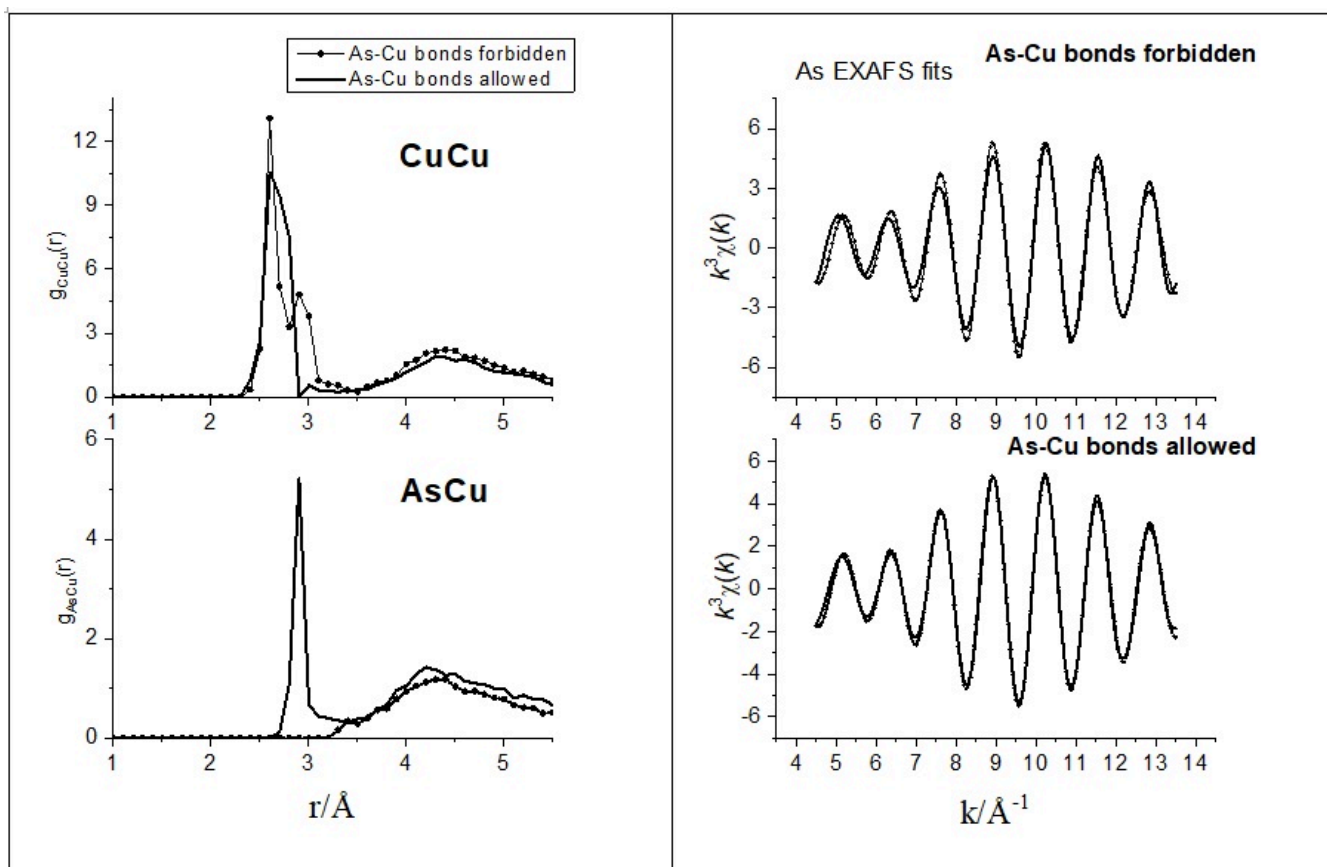


Figure 1. Comparison of As-Cu and Cu-Cu partial pair correlation functions (left) and As K-edge EXAFS fits (right) of glassy $\text{As}_{20}\text{Cu}_{20}\text{Te}_{60}$ obtained with and without As-Cu bonds

The presence of Cu-As bonds was proven by dedicated simulation runs. In Figure 1, we compare the Cu-Cu and Cu-As partial pair correlation functions and the $\text{As}_{20}\text{Cu}_{20}\text{Te}_{60}$ As K-edge fits obtained with and without Cu-As bonds. Two observations can be made here: i) the fit quality worsens upon eliminating Cu-As bonding, ii) a secondary Cu-Cu peak appears in the Cu-Cu partial pair correlation function to compensate for the lack of the Cu-As peak. This secondary Cu-Cu peak is necessary to maintain at least the Cu K-edge EXAFS fit quality. The presence of As-Cu bonds was verified by dedicated simulation runs. The Cu-Te bond length is $2.57 \pm 0.02 \text{ \AA}$ while the Cu-As distance is as high as $2.86 \pm 0.04 \text{ \AA}$. The results further showed that besides As and Te, Cu atoms also bind to Cu. The total coordination number of Cu is significantly higher than 4 for $x = 25$ and 30.

Temperature dependent structure and dynamics of ethanol-water mixtures at low alcohol contents. – By making use of literature X-ray diffraction data, extensive molecular dynamics computer simulations have been conducted for ethanol-water liquid mixtures in the water-rich side of the composition range, with 10, 20 and 30 mol % of the alcohol, at temperatures between room temperature and the experimental freezing point of the given mixture. All-atom type (OPLS) interatomic potentials have been assumed for ethanol, in combination with two kinds of rigid water models (SPC/E and TIP4P/2005). Both combinations have provided excellent reproductions of the experimental X-ray total structure factors at each temperature; this provided a strong basis for further structural analyses. Beyond partial radial distribution functions, various descriptors of hydrogen bonded assemblies, as well as of the hydrogen bonded network have been determined from the simulated particle configurations. A clear tendency was observed towards that an increasing proportion of water molecules participate in hydrogen bonding with exactly 2 donor- and 2 acceptor sites as temperature decreases. Concerning larger assemblies held together by hydrogen bonding, the main focus was put on the properties of cyclic entities: it was found that, similarly to methanol-water mixtures, the number of hydrogen bonded rings has increased with decreasing temperature. However, for ethanol-water mixtures the dominance of not the six-, but of the five-fold rings could be observed (see Figure 2).

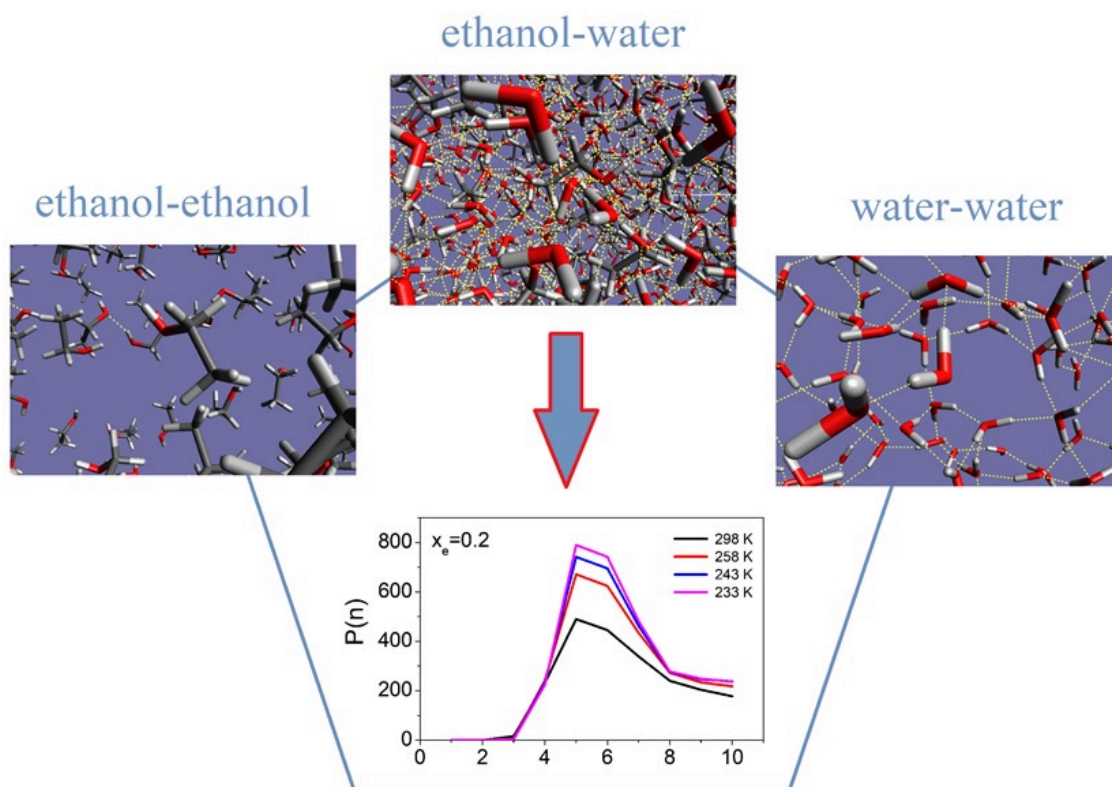


Figure 2. Temperature dependence of hydrogen bond ring size distribution in water-20 mol% ethanol mixture

Starting from the molecular dynamics simulations mentioned above, we took a closer look at the time-dependent behavior of molecules. Temperature dependent hydrogen bond energetics and dynamical features, such as the diffusion coefficient and reorientational times, have been determined for ethanol-water mixtures with 10, 20 and 30 mol % of ethanol. Concerning pairwise interaction energies between molecules, it was found that water-water interactions become stronger, while ethanol-ethanol ones become significantly weaker in the mixtures, than the corresponding values characteristic to the pure substances. Concerning the diffusion processes, for all concentrations the activation barrier of water and ethanol molecule become very similar to each other. Reorientational motions of water and ethanol become slower as ethanol concentration is increasing. Characteristic reorientational times of water in the mixtures are substantially longer than these values in the pure substance. On the other hand, for ethanol this change is only moderate. Reorientational motions of water (especially the ones related to the H-bonded interaction) become very similar for those of ethanol in the mixtures.

The structure of the simplest liquid aldehydes. – Although aliphatic aldehydes (a.k.a. alkanals, compounds with chain-end $-\text{CHO}$ groups) constitute an essential group of organic substances, structural studies of them are scarce. Synchrotron X-ray diffraction experiments and molecular dynamics simulations have been performed on simple aliphatic aldehydes in the liquid state, from propanal to nonanal. The performance of the OPLS all-atom interaction potential model for aldehydes has been assessed via direct comparison of simulated and experimental total scattering structure factors. In general, MD results reproduce the experimental data at least semi-quantitatively. However, a slight mismatch can be observed between the two datasets in terms of the position of the main diffraction maxima. Partial radial distribution functions (PRDF) have also been calculated from the simulation results. Clear differences could be detected between the various O-H partial radial distribution functions, depending on whether the H atom is attached to the carbon atom that is doubly bonded to the oxygen atom of the aldehyde group or not. Based on the 3 different O-H PRDF-s, as well as on the various H-H PRDF-s, it may be suggested that neighboring molecules turn toward each other (somewhat) preferentially by their aldehyde ends. From $g_{\text{OO}}(r)$ and $g_{\text{C}^{\text{C}}}(r)$, and from intermolecular angular correlations presented in Figure 5, it may be discerned that no (or at most, extremely weak) orientational correlations are present between neighboring aldehyde groups.

As a follow-up of the above series of experiments, the total scattering structure factors of pure liquid n-pentanol, pentanal, and 5 of their mixtures have been determined by high energy synchrotron X-ray diffraction experiments. For the interpretation of measured data, molecular dynamics computer simulations were performed, utilizing 'all-atom' type force fields. The diffraction signals in general resemble each other over most of the monitored scattering variable, Q , range above 1 \AA^{-1} , but the absolute values of the intensities of the small-angle scattering maximum ('pre-peak', 'first sharp diffraction peak'), around 0.6 \AA^{-1} , change in an unexpected fashion, non-linearly with the composition. MD simulations are not able to reproduce this low- Q behavior; on the other hand, they do reproduce the experimental diffraction data above 1 \AA^{-1} rather accurately. Partial radial distribution

functions are calculated based on the atomic coordinates in the simulated configurations. Inspection of the various O-O and O-H partial radial distribution functions clearly shows that both the alcoholic and the aldehydic oxygens form hydrogen bonds with the hydrogen atoms of the alcoholic OH-group.

Aqueous salt solutions. –Highly concentrated aqueous lithium chloride solutions have been investigated by classical molecular dynamics (MD) and reverse Monte Carlo (RMC) simulations. At first MD calculations have been carried out applying twenty-nine combinations of ion-water interaction models at four salt concentrations. The structural predictions of the different models have been compared, the contributions of different structural motifs to the partial pair correlation functions (PPCF) have been determined. Particle configurations obtained from MD simulations have been further refined using the RMC method to get better agreement with experimental X-ray and neutron diffraction data. The PPCFs calculated from MD simulations have been fitted together with the experimental structure factors to construct structural models that are as consistent as possible with both the experimental results and the results of the MD simulations. The MD models have been validated according to the quality of the fits. Although none of the tested MD models can describe the structure perfectly at the highest investigated concentration, their comparison made it possible to determine the main structural properties of that solution as well. It was found that four nearest neighbors (oxygen atoms and chloride ions together) are around a lithium ion at each concentration, while in the surroundings of the chloride ion hydrogen atom pairs are replaced by one lithium ion as the concentration increases. While in pure liquid water four water molecules can be found around a central water molecule, near the solubility limit nearly all water molecules are connected to two chloride ions (via their hydrogen atoms) and one lithium ion (by their oxygen atoms).

2017

Understanding disordered structures. — Our research group is involved in the investigation of short-range order of liquids, amorphous materials and disordered crystals. We combine experimental data such as X-ray and neutron diffraction structure factors and EXAFS spectra with computer modeling tools such as Reverse Monte Carlo (RMC) and molecular dynamics (MD) simulations. As a result of such an approach, large configurations (typically tens of thousands of atoms) are provided that are energetically reasonable and consistent (within errors) with experimental data. These configurations are then subjected to various geometrical analyses, so that specific questions concerning the structure of a material may be answered. The group is also responsible for the maintenance and operation of the MTEST neutron diffractometer installed at the 10 MW Budapest Research Reactor. Below, we provide some selected results from the year of 2017.

Metallic glasses. — The structure of glassy $\text{Cu}_{47.5}\text{Zr}_{47.5}\text{Ag}_5$ has been investigated by neutron diffraction with isotopic substitution, X-ray diffraction as well as with Cu and Ag K-edge extended X-ray absorption spectroscopy (EXAFS) measurements. Experimental datasets have been fitted simultaneously with the reverse Monte Carlo simulation technique. Nearest-neighbor distances and coordination numbers have been determined and compared with those of glassy $\text{Cu}_{50}\text{Zr}_{50}$ and $\text{Cu}_{47.5}\text{Zr}_{47.5}\text{Al}_5$. It has been found that the Cu-Cu coordination number drops upon adding Al or Ag to $\text{Cu}_{50}\text{Zr}_{50}$. Both Ag and Al prefers Zr to Cu. The total coordination number of Ag is 13.9 ± 0.6 while that of Al is 10.2 ± 1.0 , suggesting that, in spite of their similar molar volumes, the effective size of Ag and Al in the Cu-Zr matrix is quite different. This is reflected both by the comparison of Zr-Al and Zr-Ag partial pair distribution functions and the Zr-X-Zr (X=Al, Ag) cosine distributions (see Fig. 1.)

Alcohol-water mixtures. — Our efforts concerning the structure of alcohol-water liquid mixtures have been extended to the study of the temperature dependence of the structure of aqueous solutions of methanol. The evolution of the structure of liquid water-methanol mixtures as a function of temperature has been studied by molecular dynamics simulations, with a focus on hydrogen bonding. The combination of the OPLS-AA (all atom) potential model of methanol and the widely used SPC/E water model has provided excellent agreement with measured X-ray diffraction data over the temperature range between 298 and 213 K, for mixtures with methanol molar fractions of 0.2, 0.3 and 0.4. Hydrogen bonds have been identified via a combined geometric/energetic, as well as via a purely geometric definition. The number of recognizable hydrogen bonded ring structures in some cases doubles while lowering the temperature from 298 to 213 K; the number of sixfold rings increases most significantly. An evolution towards the structure of hexagonal ice, that contains only sixfold hydrogen bonded rings, has thus been detected on cooling water-methanol mixtures. For a picture of typical hydrogen-bonded ring structures, see Figure 2.

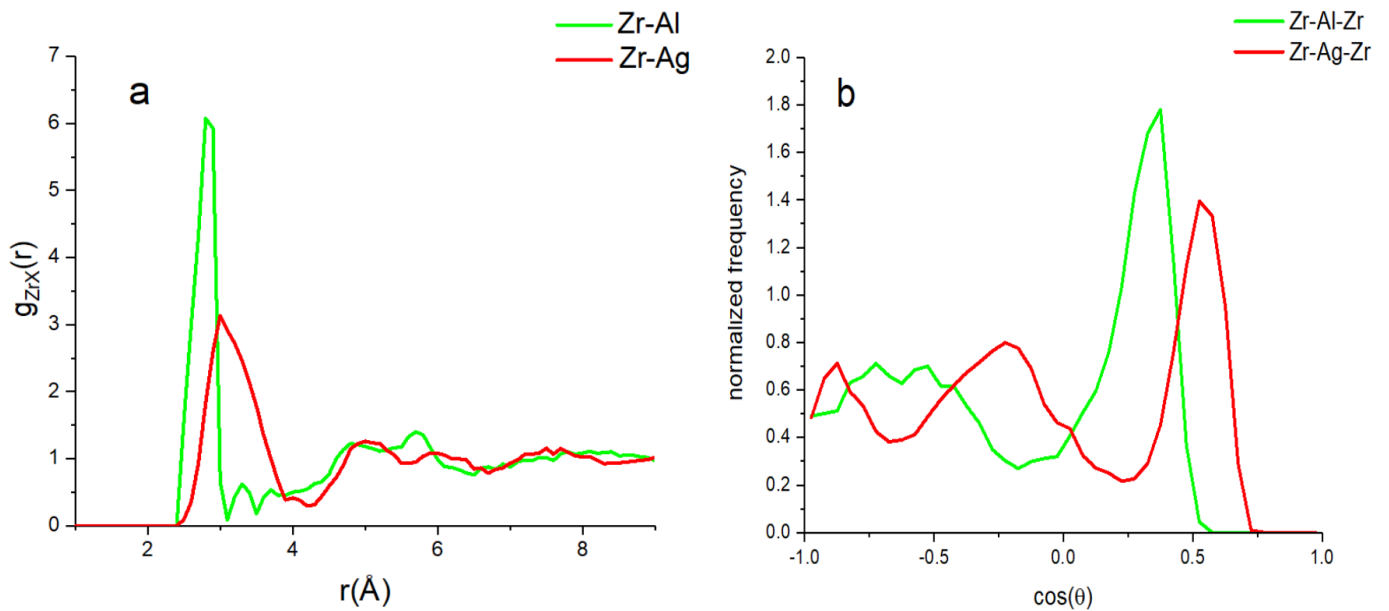


Figure 1. Effective size difference of Al and Ag atoms in the Cu-Zr host matrix as reflected by the position of the first peak of Zr-Al and Zr-Ag partial pair distribution functions (a) and by the Zr-Al-Zr and Zr-Ag-Zr cosine distributions (b)

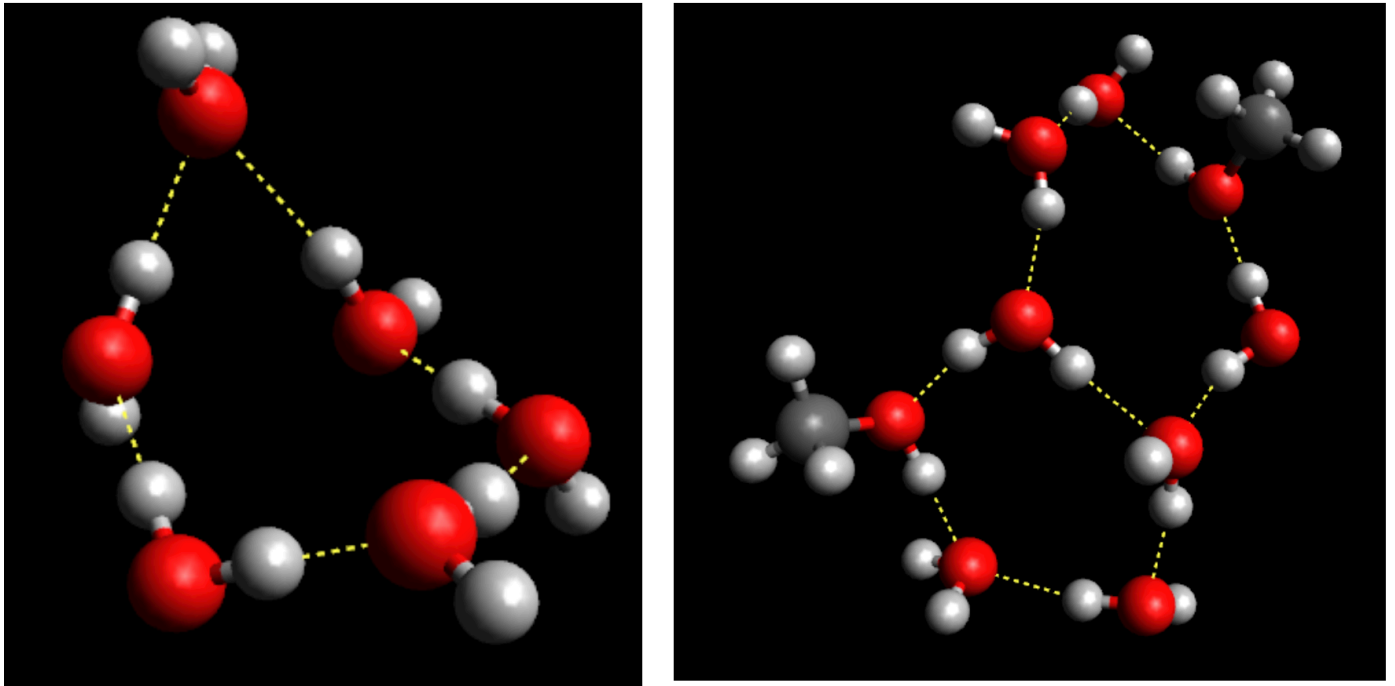


Figure 2. Hydrogen-bonded ring structures in methanol/water mixtures (Red: O atoms; light grey: H atoms; dark grey: C atoms. Dashed lines represent hydrogen bonds between molecules.)

Liquid chalcogenides. — The short-range order in the liquid state of GeTe, a prototypical phase-change material employed in data storage devices, has been investigated by X-ray and neutron diffraction in the temperature range from 1197 to 998 K. We have also measured the dynamic viscosity from 1273 to 953 K, which is 55 K below the solidification point, using an oscillating-cup viscometer. The measurements have been complemented with ab-initio molecular dynamics (AIMD) simulations based on density functional theory (DFT). Compatibility of the AIMD-DFT models with the diffraction data has been proven by simultaneous fitting of all datasets in the frame of the reverse Monte-Carlo simulation technique. It has been shown that octahedral order dominates in liquid GeTe, although tetrahedral structures are also present. The temperature dependences of the structural parameters, dynamic viscosity and electronic properties extracted from the AIMD models have been analyzed and discussed. We have shown that GeTe keeps its semiconductor nature in the liquid and supercooled liquid state. Its viscosity obeys the Arrhenius law with a small activation energy of the order of 0.3 eV, which is indicative of a highly fragile liquid.

Aqueous salt solutions. — Aqueous lithium chloride solutions up to very high concentrations have been investigated in classical molecular dynamics simulations. Various force fields based on the 12-6 Lennard-Jones model parametrized for non-polarizable water solvent molecules (SPC/E, TIP4P, TIP4PEw) have been inspected.

Twenty-nine combinations of ion-water interaction models have been examined at four different salt concentrations.

Densities, static dielectric constants and self-diffusion coefficients have been calculated (see, e.g., Figure 3). Results derived from the different force fields scatter over a wide range of values. Neutron and X-ray weighted structure factors have also been calculated from the radial distribution functions and compared with experimental data. It has been found that the agreement between calculated and experimental curves is rather poor for several investigated potential models, even though some of them were previously applied in computer simulations.

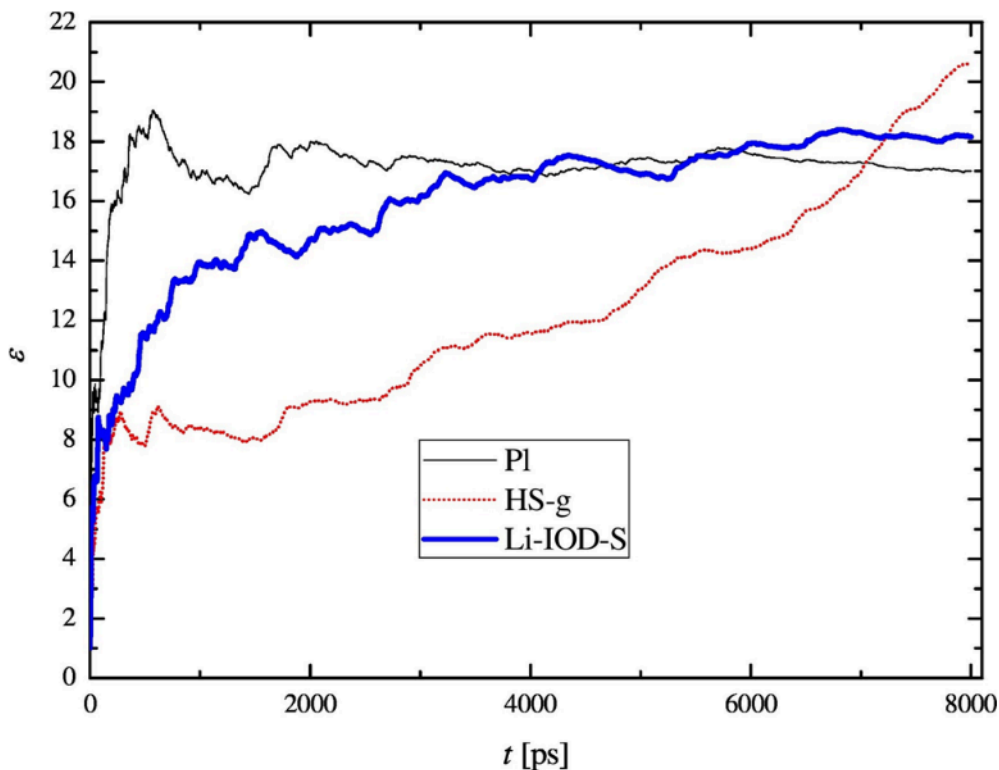


Figure 3. Convergence of the static dielectric constant (ϵ) for three selected models (PI, HS-g and Li-IOD-S) at the concentration $m = 19.55$ mol/kg. The curve is converged for the PI model, still slightly evolving for the Li-IOD-S model, and definitely not converged even at 8 ns, for the HS-g model.